PRESENTATION OF A MEASUREMENT CAMPAIGN IN UNDERGROUND RAILWAY STATIONS FOR THE VALIDATION OF A HYBRID PROPAGATION MODEL BASED ON RAY-TRACING

T I Sefsouf, Pierre Combeau, J. Arnould, Yannis Pousset

PRESENTATION OF A MEASUREMENT CAMPAIGN IN UNDERGROUND RAILWAY STATIONS FOR THE VALIDATION OF A HYBRID PROPAGATION MODEL BASED ON RAY-TRACING

T. I. SEFSOUF[1,2], P. COMBEAU[1], J. ARNOULD[2], Y. POUSSET[1]

[1]XLIM Institute, 11, Boulevard Marie et Pierre Curie, 86962 Futuroscope, France
[2]SNCF Réseau, Engineering and Projects, Telecommunications Department
6, Avenue François Mitterrand, 93754 La Plaine Saint-Denis, France
ilham.sefsouf@univ-poitiers.fr

KEYWORDS: Propagation, calibration, measurements, propagation model, railway stations

ABSTRACT

This paper presents measurement campaign conducted in some train stations in Paris (France) in order to implement and validate a hybrid propagation model in underground railway station environments. In those propagation environments, we can find many geometrical details (pillars, platforms …) and mobile details (trains and passengers) that make the behavior of the radio-waves complex for modelling as they involve multiple reflected, diffracted and scattered waves which can bring about severe degradation of the received signal. The principle of the proposed hybrid model is to combine two approaches: deterministic, based on ray-tracing approach, and statistical ones. On the one hand, the macro geometric characteristics of the train station are considered by the deterministic part; on the other hand, the statistical part considers the spatio-temporal variability (essentially due to the mobility of passengers and trains) and the details which were not considered by the deterministic part (either small objects compared to the wavelength or complex objects).

The implementation of such model requires measurement campaigns in order to calibrate the deterministic aspects of the model. This paper focuses on the calibration of a ray-tracing model using measurements carried out at 400 MHz, 700 MHz, 900 MHz, 1800 MHz, 2100 MHz and 2700 MHz.

INTRODUCTION

During the last years, many studies related to the radio waves propagation in railway scenarios have been published especially in tunnel environments. However, the propagation in train stations has been rarely investigated and there is still a lack of measurements and knowledge regarding to the propagation in those environments. When considering their complex structure, the stations have significant differences compared to other environments such as tunnels, as they involve an abundance of multiple reflected, diffracted and scattered waves. A few recent works are interested in this issue (Ke Guan et al. 2014a, Ke Guan et al. 2014b, Lei Zhang et al. 2014, Xuesong Cai et al. 2015, Lei Zhang et al. 2015a, Lei Zhang et al. 2015b, Lei Zhang et al. 2016, Xingqi Zhang et al, 2016).

Guan et al. classify the train stations into three main types: closed, semi-closed and open stations. The authors notice that "the first one is similar to typical indoor environments and could be modelled by many existing indoor models". Therefore, their work focuses on open and semi-closed stations and they propose empirical models for extra propagation loss based on measurements conducted in the railway stations in China; "Luo Yang Nan" and "Ling Bao Xi". In (Xingqi Zhang et al. 2016), the authors develop a hybrid ray tracing/vector parabolic equation for modelling the radio propagation for the train communication channels. The ray tracing is applied to the complex geometries (such as railway stations) and the vector parabolic equation is applied to the uniform tunnels. They validate their model in the railway station of Edmonton, Canada. They calibrate in (Xingqi Zhang et al. 2015a, Xingqi Zhang et al. 2015b) the ray-tracing model presented in (Neeraj Sood et al, 2011) by ascertaining optimal values for the input parameters.

In (Lei Zhan et al.2015a and Lei Zhang et al 2015b), the authors focus their studies on the broadband measurements conducted in line 3 of the Madrid subway station, more precisely, in the subway tunnel, the station and the transition between the tunnel and the station. They conclude that the subway station, which is covered with steel panels, is a dense multipath environment compared to tunnels where the multipath components are reduced by the filtering effect of the tunnel. Moreover, they also conclude that the movement of the train in the station has small impact on the delay spread. In last, they demonstrate that the propagation in subway stations at the frequencies 2,4GHz and 5,7 GHz is more suitable than that at 1000 MHz and 900 MHz, because the propagation at 900 MHz and 1000 MHz has much longer root mean square (RMS) delay spread and has more multipath components than at 2,4 GHz and 5,7 GHz.

These results matched other studies (Lei Zhang et al.2016) conducted at 950 MHz and 2150 MHz in a semi-closed high-speed station covered with steel roof (Da-Xi High Speed Railway, Shanxi Province, China). The results matched the measurements conducted in (Xuesong Cai, 2015) at 2132, 6 MHz in the subway platform and tunnel of the Metro Line 11 Shanghai, China. The purpose of these measurements is to study differences between radio wave propagation channels in both train platform and tunnel scenarios. The authors conclude that the delay spread on the platform is four times larger than that in tunnels. Furthermore, they observe that there were more than three dense multipath components (DMC) on the train platform and only one in the tunnel.

All those studies conclude that the stations represent a high-multipath environment leading to more complex scenarios than tunnels. Moreover, the existing studies are generally related to train communication/control systems for which the receiver systems are installed in the train. Unlike these studies, we focus our works on underground train stations, where many radio systems (GSM, UMTS, LTE, TETRA, TETRAPOL…) are deployed to guarantee services to the passengers of the station, security and rescue forces, and railway agents. The radio engineering needed to set up those radio networks, requires a suitable propagation model to estimate the radio coverage in train stations. Currently, these estimations are mainly based on on-site measurements conducted by the Telecommunications Department of “France’s SNCF RESEAU Engineering and Projects”, which are expensive and difficult to extrapolate to other stations.

Measurement is an accurate method for dimensioning radio networks but it remains costly and requires significant human and material resources; simulation is a good alternative to measurements, providing that a suitable propagation model is used. Providing a specific model to station environments is an important issue for SNCF in order to limit the measurement campaigns, which are currently the only reliable method for establishing communication means at stations.

In a typical railway station, we can find many details in the propagation environment such as pillar, etc. From the point of view of wave propagation, those objects can block parts of line of sight (LOS) between the receiver and the transmitter. Furthermore, passengers and trains make the behaviour of the propagation even more complex for modelling by aggravating the fading behaviour.

In this paper, we present analysis of narrowband measurements conducted in two train stations in Paris (France): “Avenue Henri Martin” and “Paris Austerlitz”. Those underground stations are on line C of the regional express network “RER”; the commuter rail service serving Paris and its suburbans.

The remainder of this paper is structured as follows. The measurement environments are descripted in the second section. The third section exhibits the measurements. The analysis of the measurements and simulations is presented in the fourth section. Finally, a conclusion is drawn.

DESCRIPTION AND CLASSIFICATION OF THE ENVIRONEMENT

Station configurations vary greatly in size, shape, architecture, materials, and passenger flow rate. Nevertheless, we can classify those environments into two typical zones, “platform zone” and “exchange zone”. These areas are not only characterized by their particular geometry but also by the specific type of elements responsible for the temporal variability, such as the presence of trains only in the platform zone.

The main geometrical elements of the platform zone are: train platforms, railway tracks, wall niches, pillars and benches. The arrangement of the rail tracks with respect to the train platforms can be divided into three categories: a central platform overlooking two rail tracks on either side (Figure 1 (a)), two juxtaposed central rail tracks separating the train platforms (Figure 1(b)), and alternating train platforms and rail tracks (Figure 1(c)). On the other hand, the form of the station can be curved (Figure 2(a)) or rectangular (Figure 2(b)).

As for them, the exchange zones have open halls, corridors and commercial shops. In both zones, we can also find stairs/escalators, billboards (information, lighting, and advertising) and passengers.

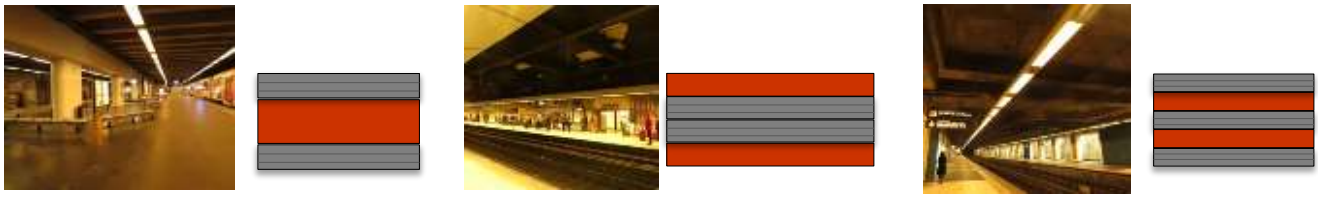

(a) (b) (c)

Fig.1 Platform Zone

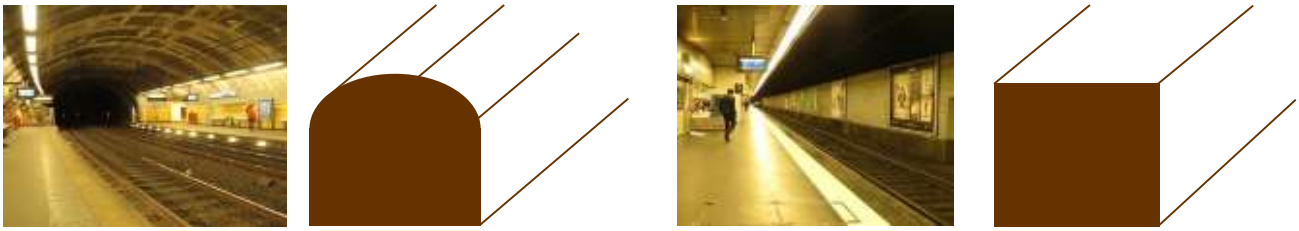

(a) (b)

Fig. 2 Form of the station

Based on this classification, the measurement campaign was performed in the platform zone of “Avenue Henri Martin” and in the exchange zone of “Paris Austerlitz”.

DESCRIPTION OF THE MEASUREMENTS

The transmission system, as shown in figure 3, is composed of an RF signal generator ANRITSU S3332E, connected by a low-loss coaxial cable RG214 to a vertically polarized dipole antenna of 2dBi gain KATHEREIN 737003 or 80020847 (depending on frequency) installed on a tripod mast . The transmission is in a continuous mode on the following carrier frequencies: 400 MHz, 700 MHz, 900 MHz, 1800 MHz, 2100 MHz and 2700 MHz.

Fig.3 Transmission System

The reception system is placed in a backpack as illustrated in Figure 4. The measurement acquisitions are monitored by a laptop via the software ROMES developed by Rohde &Schwarz. The laptop is connected to the RF receiver TSMU 1153.6000.02 Rohde & Schwarz which is connected via a low-loss coaxial cable RG58A/U to a vertically polarized dipole antenna identical to the one in the transmission system. Furthermore, the laptop is also connected to a tachometric wheel that allows us to acquire regularly spaced measuring points with a minimum step of 2 cm.

Fig.4 Reception System

The measurements are carried out on foot on predefined paths, which are plotted in advance on the plans of the stations. The measurements points were marked on the ground using a laser meter in order to re-conduct the same measurement paths for the six considered frequencies.

The objective of the measurement is to analyse the evolution of the received power on a predefined path and to compare it with the simulation carried out in the same configuration.

The received signal in a spatial domain can be expressed as follows:

$$r(x) = m(x).r_0(x)$$

Where $r(x)$ is the received signal, $r_0(x)$ is the small scale fading and $m(x)$ is the local average power, which represents the large-scale propagation characteristics, including both path loss and shadow fading.

To obtain the local average power, we have to eliminate the small scale fading in the received signal by averaging out over a distance. The required averaging distance is determined to be in the range of twenty to forty wavelengths (20λ-40λ) in accordance with Lee criterion (William C.Y LEE, 1985). The minimum required number of samples must be 36 and these samples must be uncorrelated. To respect these two conditions, the separation distance between two adjacent samples must be within the range of 0,8λ and 1,11 λ.

For our measurements, we choose to take a separation of λ between our samples, and then we average out over a length of 40λ.

MEASUREMENTS, SIMULATIONS AND ANALYSIS

SCENARIO 1 : Platform Zone « Avenue Henri Martin Station »

The platform zone of "Avenue Henri Martin" station is rectangular and composed of alternating two train platforms and three rail tracks. It is also composed of pillars along the platforms as illustrated in figure 5. The transmitter system is placed at the end of the platform, the transmitting antenna is placed at a height of 3m and the measurements are carried out on foot along the platform.

The measurements were carried out at 400 MHz, 700 MHz, 900 MHz, 1800 MHz, 2100 MHz and 2700 MHz. The figure 5 illustrates the transmitter and the receivers' positions.

Fig 5. Transmitter and receivers' positions

The transmit powers that the generator delivered are measured using a spectrum analyser. Table 1 gives the transmit power values for each frequency:

Frequency	Power (dBm)
400 MHz	5,05
700 MHz	4,09
900 MHz	3,73
1800 MHz	-1,2
2100 MHz	-1,46
2700 MHz	-0,27

Table 1. Measured Power

The main elements to be modelled in this station are platforms, rail tracks, walls, ceiling, pillars. Wall niches are present throughout the walls. Let "structure" refers to all the walls, platforms and ceiling. The incremented details to our structure are the niches, which are present throughout the walls, and the pillars, which are present throughout the two platforms as shown in Figure 6.

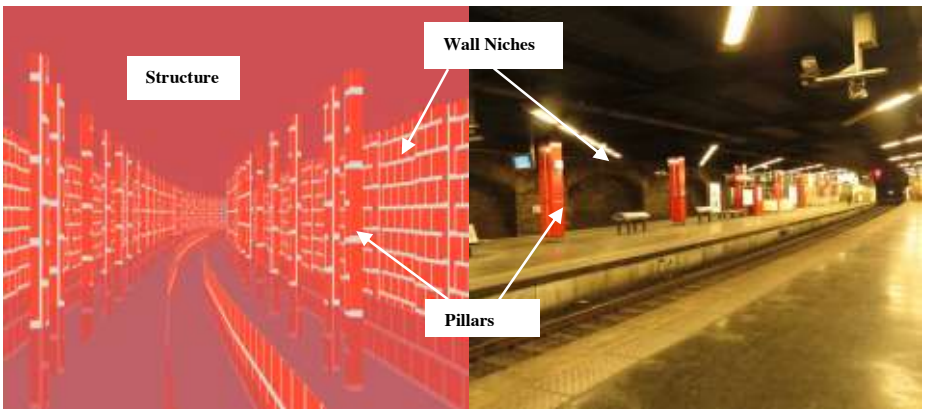

Fig. 6 A 3D Modelling

Simulations are carried out with a 3D ray-tracing tool combined to Geometrical Optics laws. We have implemented in the simulator the real radiation patterns of the antennas. The radiation patterns were measured in an anechoic chamber for the six frequencies. The figure 7 (a) shows the radiation pattern of the antenna “KATHEREIN 80020847” and the Figure 7 (b) shows the radiation pattern of the antenna “KATHEREIN 737003”.

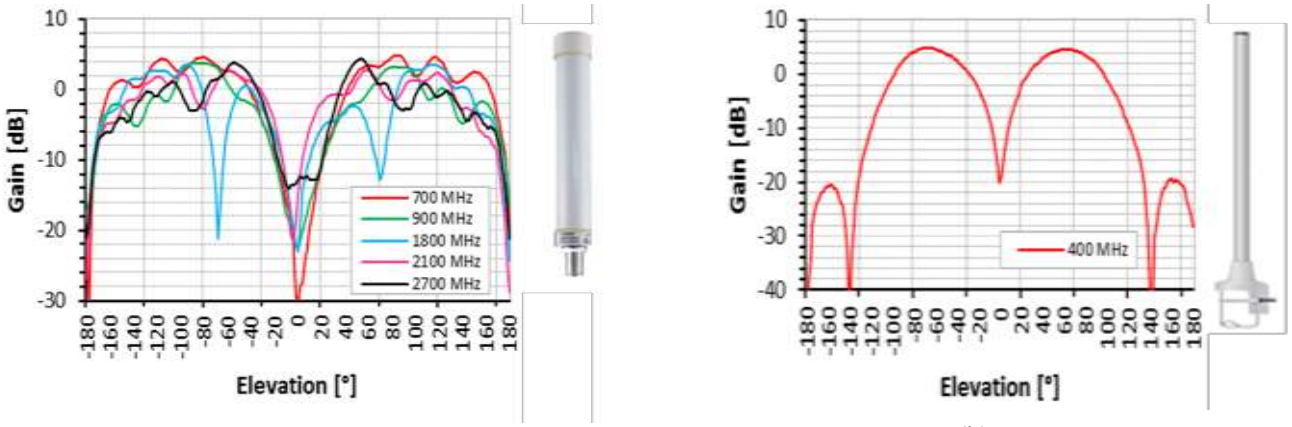

(a) (b)

Fig. 7 Radiation Patterns

In the following analysis, we calibrated the number of interactions necessary for the convergence of the simulation results, and to ensure that a trade-off between execution time and accuracy is achieved. Firstly, we increased the number of reflexions to ten reflections. Then, we added diffraction to our simulations. In addition, we added a transmission to the reflections, because in the non-line of sight (NLOS) zones, especially at the end of the platform, the reflected paths cannot reach the receiver unless we consider a large number of reflections (e.g. 10 reflections). Let “R” refers to the reflection, “T” to the transmission and “D” to the diffraction.

The simulation curves, which have been smoothed in accordance to the Lee criterion described above, are given in the Figure 8(a) with a various number of reflections (and one transmission).Their Cumulative Distribution Functions (CDFs) are given in the Figure 8(b). The figures show that the simulation results converge with three reflections. This trend is observed for all frequencies. This can be explained by the fact that the predominant path is the direct path for most receivers. However, for the receivers at the end of the curve, which are in NLOS zone, we can see the impact of the transmission when considering the curve 10R and the other curves, which combine a transmission with reflections.

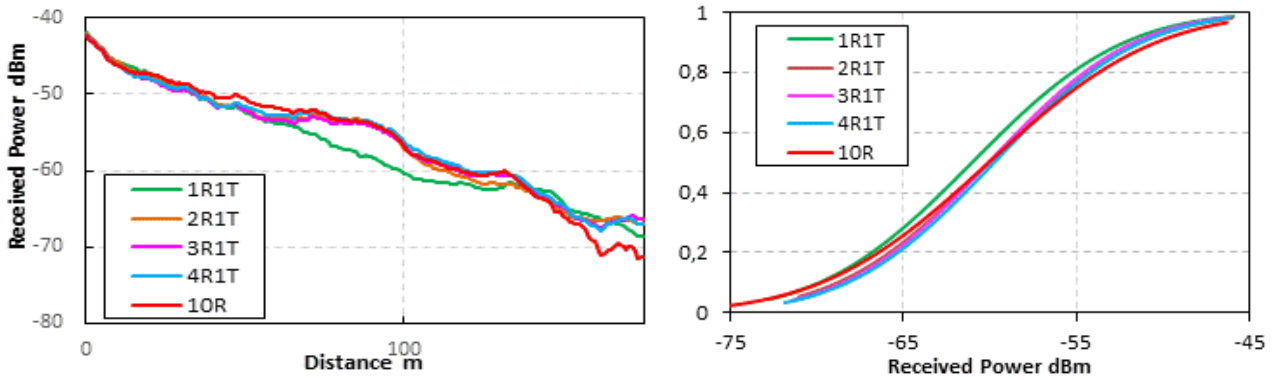

(a) (b)

Fig. 8 Received power and CDF with a various number of interactions

In the following results, we will see the impact of the diffraction as a function of frequency by comparing the simulation results with the measurements. Results are given in Figure 9 ((a) to (f)).

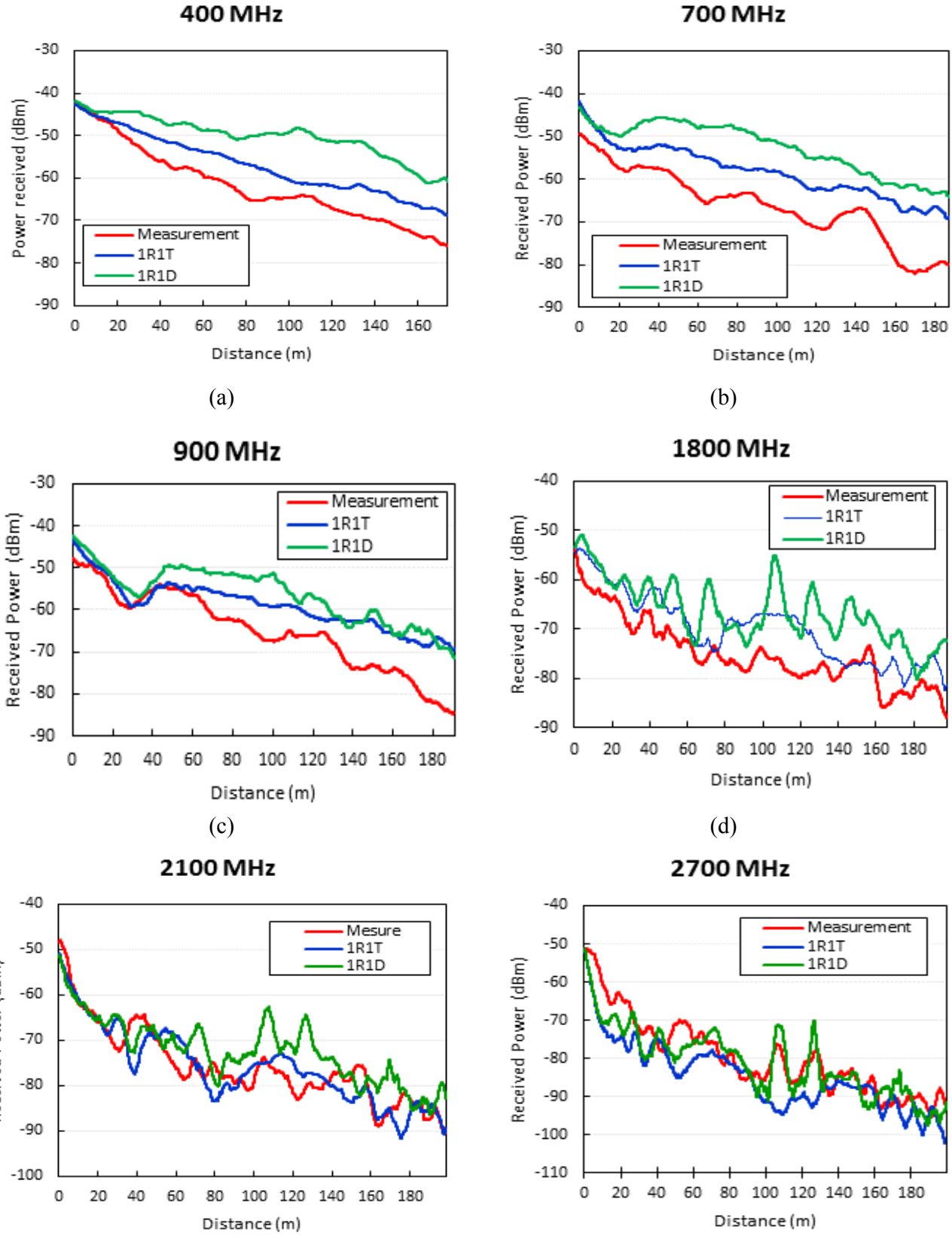

Fig.9 Impact of Diffraction

The diffraction can increase the received signal level for the low frequencies, we can see in table 2 that the mean error is doubled, this can be explained by the fact that the configuration is mainly in LOS. This can be also justified by the fact that the asymptotic method is a high frequency technique. On the other hand, for high frequencies, the attenuation due to diffraction is much greater than that due to reflection. In this case, diffraction is an important propagation mechanism. For example, at 2700 MHz diffraction gives better results, i.e. the mean error is less than that with a reflection and transmission. (Table 2).

	1R1T		1R1D	
	Mean Error (dB)	Standard Deviation (dB)	Mean Error(dB)	Standard Deviation (dB)
400 MHz	5,04	2,12	11,88	4,69
700 MHz	7,85	2,96	13,51	3,97
900 MHz	6,13	4,23	8,77	4,21
1800 MHz	5,28	2,93	6,62	3,99
2100 MHz	3,22	2,96	4,85	3,57
2700 MHz	5,74	4,41	4,41	2,72

Table 2 Comparison with interactions

In the following results, we are interested in the geometrical details; the objective is to determine what level of details should be considered and how these details should be modelled.

In order to observe the impact of the geometrical details on the propagation, we perform four modelling starting from the simplest to the most complete. We add incremental details to our structure; these details are niches along the walls and pillars along the platforms as shown previously in the Figure 6.

Results at 2100 MHz are given in the Figures 10(a) and 10(b) for 1R1T and 3R1T respectively. The more we add details in our environment, the more the precision is. But the pillars are found to be the main objects impacting the propagation compared to the niches, if we add niches to the configuration structure + pillars, the computational time is increased and the mean error is not improved as given in table 3.

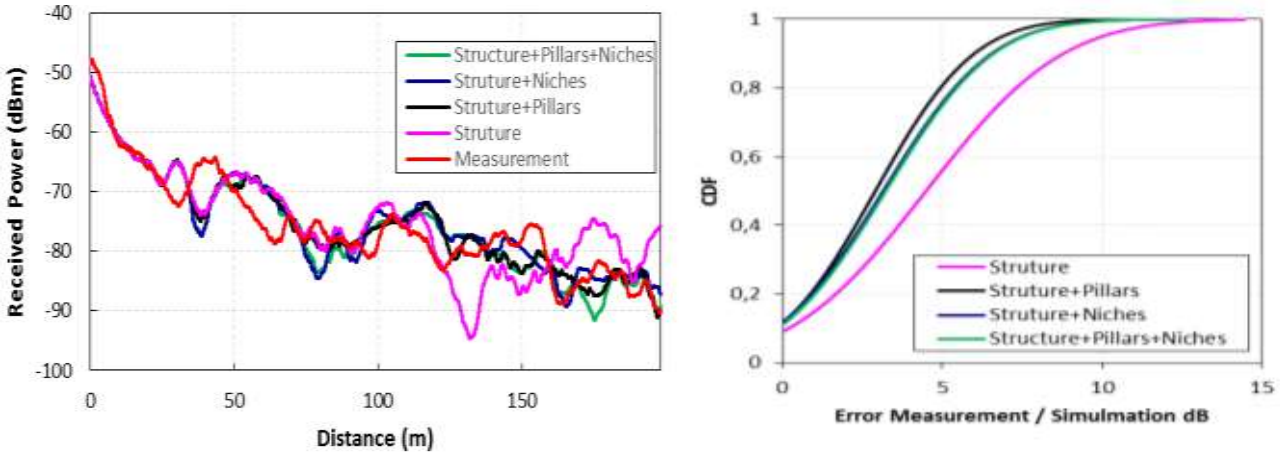

(a)

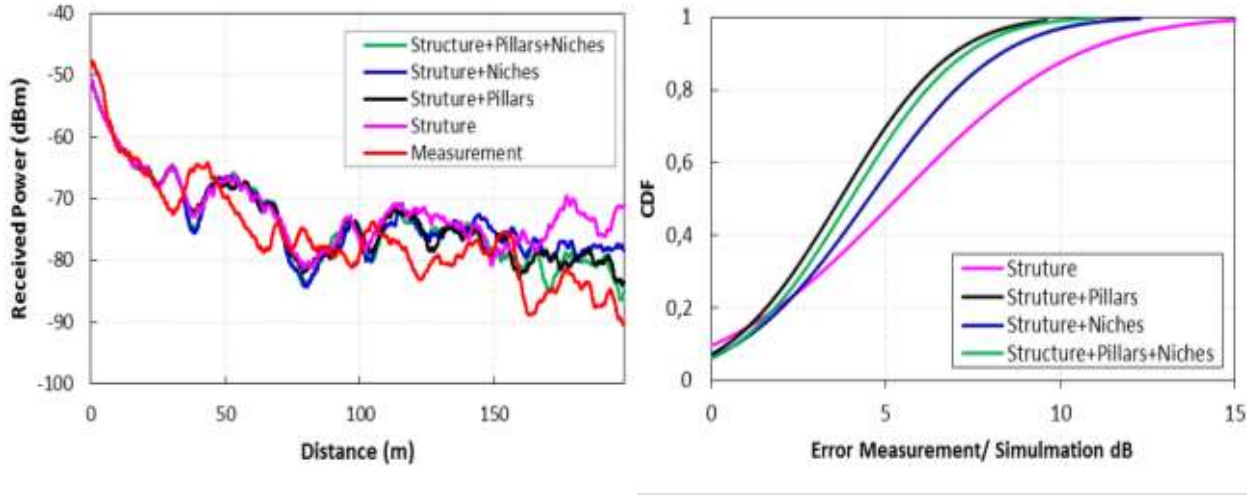

(b)

Fig. 10 Received Power with various geometrical modelling

	1R1T			3R1T		
	Mean Error	Standard Deviation	Computational Time	Mean Error	Standard Deviation	Computational Time
Struture	4,49	3,35	1s 574ms	5,31	4,07	1mn 0s 637ms
Struture+Niches	3,15	2,65	2s 481ms	4,50	2,95	4mn 19s130ms
Struture+Pillars	**2,90**	**2,41**	**2s 481ms**	**3,69**	**2,52**	**4mn 28s 157ms**
Struture+Niches+Pillars	3,22	2,63	3s 803ms	4,00	2,57	7mn 57s147ms

Table 3. Comparison with various geometrical modelling

Other factors can increase the degree of the uncertainty when comparing the measurements with the simulation, such as the exact position of the receiver measurement points because the receiver antenna is installed on a backpack. Moreover, unique dielectric properties of materials were used for modelling the whole station. In fact, the whole station is assumed to be concrete with relativity permittivity ε_r==9, and conductivity σ=0,01S/m. Figure 11 shows simulations with different values of relativity permittivity and conductivity. We note that in the region where the LOS is dominant, the results converge. However, at the end of the platform, where the receivers are in NLOS zone, the results differ, especially in low frequencies. This difference is due to the fact that the transmitted paths are strongly impacted by the nature of materials.

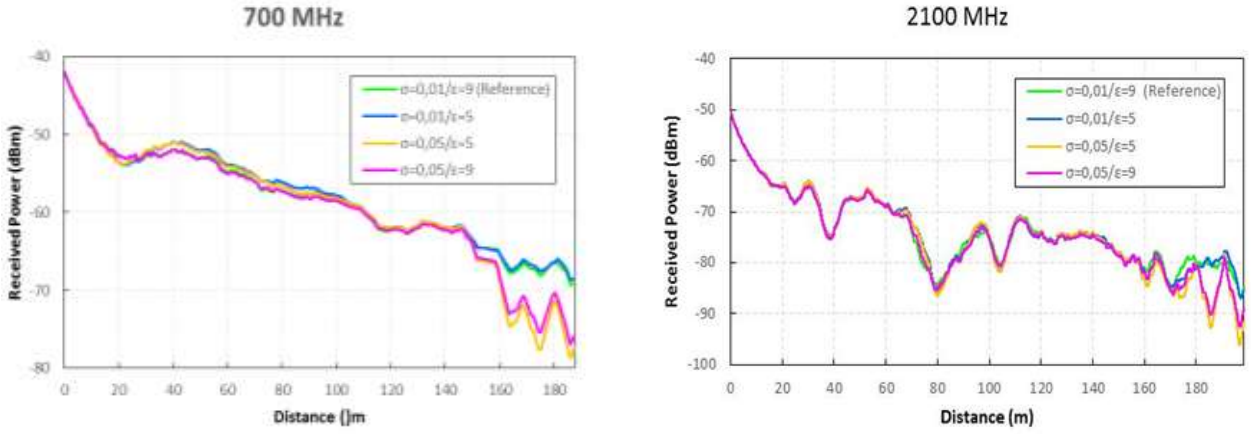

Fig.11 Received Power with various electrical parameters

To quantify the uncertainty related to the receivers' positions, we will present some results of measurements and simulations. We carried out measurements and simulations on a predefined path and then we shifted this path by 60 cm to the left and 60 cm to the right to observe the spatial variability. The results are given in the table 4. The absolute mean error can reach up to 5,5 dB, this means that if the measurement path does not correspond precisely to the simulation path, a significant error can be introduced between the measurement and the simulation. We take as an example the two extreme frequencies 400 MHz and 2700 MHz as shown in the table 4.

	Frequency (MHz)	Measurements (dB)	Simulations (dB)
Receiver position 60cm (left)	400	4,4	4,4
	2700	5	4,4
Receiver position 60cm (right)	400	4,9	4,9
	2700	5,5	4,9

Table 4. Absolute Mean Error

On other hand, the orientation of the receiver antenna might be slightly inclined while walking, simulations with an orientation of 30° shows an absolute mean error within 2dB for 400 MHz and 6 dB for 2700 MHz.

All these uncertainties can explain the error and offsets observed in the curves above shown in the Figure9.

SCENARIO2 : Exchange Zone « Paris Austerlitz Station »

This zone is composed of two parts; the first part consists of a large hall where there are commercial shops. The hall overlooks corridors with stairs and escalators allowing connections with other lines. The second part has access to the stairs to reach the platforms A et B of RER line C. We note the presence of pillars in both parts. In the first part, we carried out measurements and simulations on path 1, path 2 and path 3 as shown in the Figure 12. In the second part, measurements and simulations are conducted on path A and path B. The transmitter is placed in the centre of the hall at a height of 2,50 m as shown in the Figure 12.

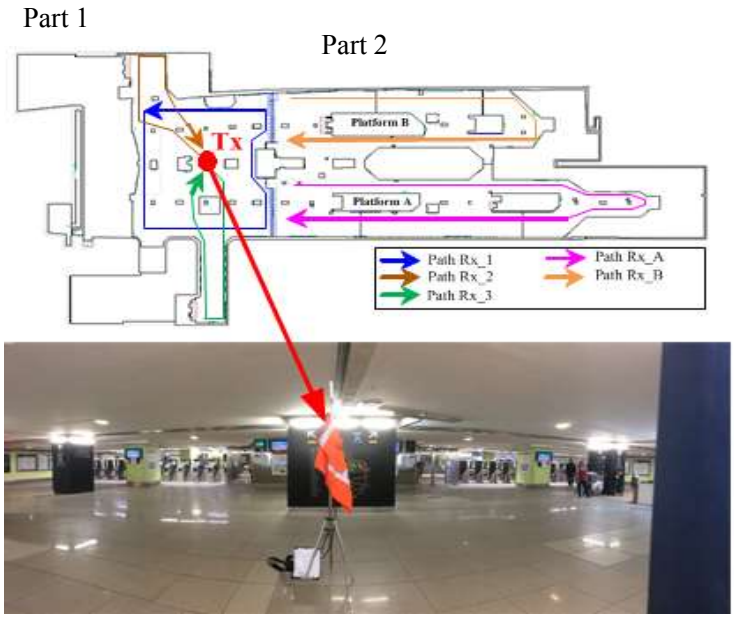

Fig.12 Receivers' Paths

We will present the results of the measurement and simulations at 2100 MHz carried out on the five paths, as shown in the Figure 13.

The Paths A and B are in the NLOS zones, we notice that the more we increase the number of reflections, the better the results. The mean error can be reduced to six times by taking account ten reflections instead of one reflection and four transmissions (Table 5). On the other hand, considering a diffraction gives good results for Path A and better results for Path B. For the Path 1, Path 2 and Path3, where a part of receivers is in LOS zone, the results converge with three reflections and two transmissions, and the association with diffraction gives better results. The table 5 shows the absolute mean error and standard deviation for all interactions.

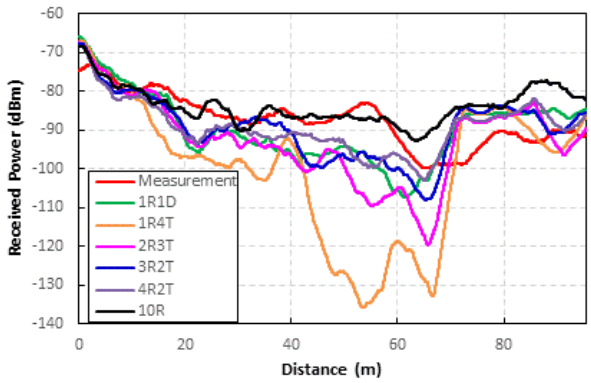

Path A

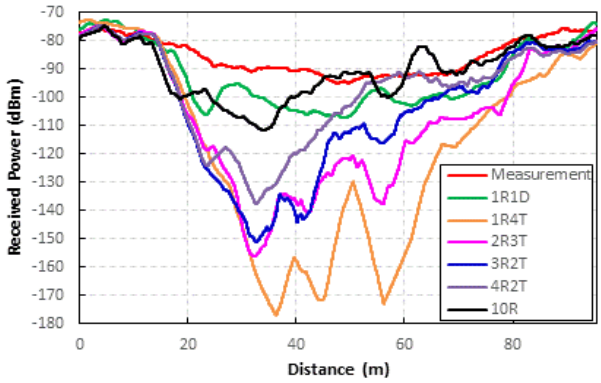

Path B

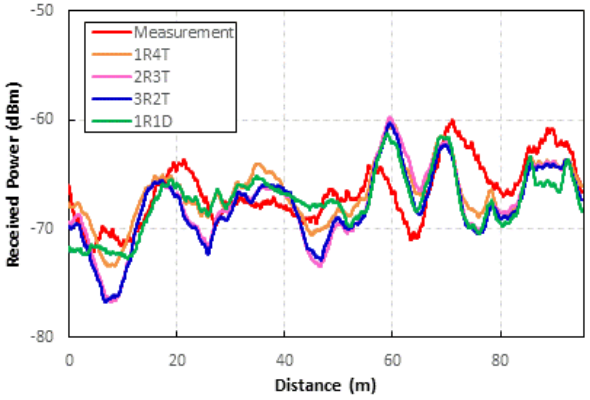

Path 1

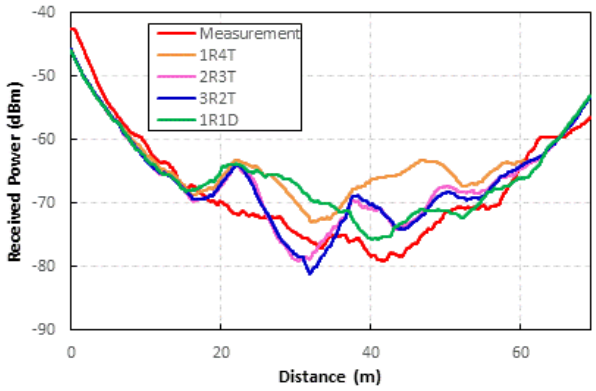

Path 2

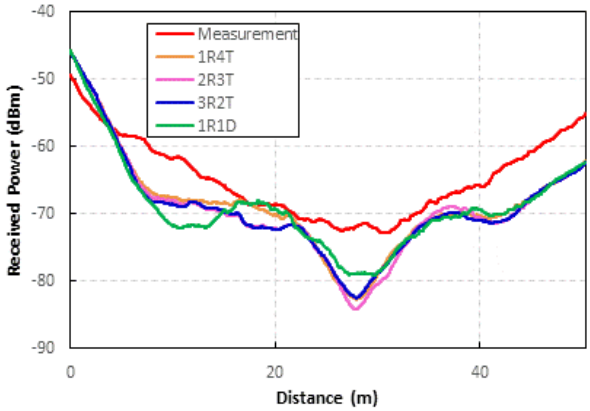

Path 3

Fig.13 Mesurements ans simulations at 2100 MHz

Interactions	Mean Error (dB)	Standard Deviation (dB)
Path1		
1R4T	2,09	1,43
2R3T	2,60	1,91
3R2T	2,53	1,84
1R1D	2,17	1,56
Path2		
1R4T	4,76	3,72
2R3T	2,95	1,88
3R2T	2,88	1,96
1R1D	3,26	2,26
Path3		
1R4T	4,05	2,48
2R3T	4,24	2,62
3R2T	4,13	2,46
1R1D	3,85	2,74
Path A		
1R4T	15,26	13,82
2R3T	8,23	6,09
3R2T	6,12	2,46
4R2T	5,60	3,93
10R_RLtoRT	5,08	4,61
1R1D	6,79	3,84
Path B		
1R4T	33,80	26,94
2R3T	22,86	17,97
3R2T	18,76	18,25
4R2T	12,56	13,69
10R_RLtoRT	6,84	6,20
1R1D	3,85	2,74

Table 5. Comparison with various interactions

CONCLUSION

In this paper, we have presented a measurement campaign in some underground railway stations, in order to calibrate simulations based on ray tracing. Narrowband analysis is presented for different zones of the stations taking into account the impact of geometrical modelling and different interactions. The results will be used to develop a hybrid propagation model based on two approaches: deterministic and statistical ones. The deterministic part, which is described in this paper, takes into account the macro geometric characteristics of the train station.

REFERENCES

Ke Guan, Zhangdui Zhong, Bo Ai and Thomas Kurner: Empirical Models for Extra Propagation Loss of Train Stations on High-speed Railway, IEEE Transactions on Antennas and Propagation, Vol. 62; No 62, pp. 1395-1408, 2014.

Ke Guan, Zhangdui Zhong, Bo Ai and Thomas Kurner : Propagation Measurements and Analysis for Train Stations of High-Speed Railway at 930 MHz, IEEE Transactions on Vehicular Technology, Vol. 63, No 8, pp. 3499-3516, 2014.

Lei Zhang, Jianwen Ding, Bei Zhang, Cesar Briso Rodriguez, Ke Guan : Measurement and Analysis Broadband Radio Propagation in a High-speed Railway Station, IEEE 83rd Vehicular Technology Conference (VTC spring),15-18 May 2016.

Lei zhang, Cesar Briso, Jean Raphael Olivier Fernandez, José I Alonso, Carlos Rodriguez, Juan Moreno Garcia-Loygorri and Ke Guan : Delay Spread and Electromagnetic Reverberation in Subway Tunnels ans Stations, IEEE Antennas and Wireless Propagation Letters, Vol.15, pp. 585-588, 2016.

Lei zhang, Jean Raphael Fernandez, Cesar Briso Rodriguez, Carlos Rodriguez, Juan Moreno and Ke Guan : Broadband Radio Communications in Subway Stations and Tunnels, 9th European Conference on Antennas and Propagation (EuCAP), 13-17 April 2015.

William C; Y. Lee: Estimate of Local Average Power of a Mobile Radio Signal IEEE Transactions on Vehicular Technology, Vol. VT-34, No 1, pp. 22-27, 1985.

Xingqi Zhang, Neeraj Sood, Joseph K. Siu and Costas D. Sarris : A Hybrid Ray-Tracing/Vector Parabolic Equation for Propagation Modeling in Train Communication Channels, IEEE Transactions on Antennas and Propagation, Vol. 64, No 5, pp. 1840-1849, 2016.

Xingqi Zhang, Neeraj Sood, Joseph Siu and Costas D. Sarris: Calibration of a 3-D Ray Tracing Model in Railway Environments, 2015 IEEE International Symposium on Antennas and Propagation & USNC/URSI National Radio Science Meeting, pp. 89-90, 19-24 July 2015.

Xingqi Zhang, Neeraj Sood, Joseph Siu and Costas D. Sarris : Efficient Propagation Modeling in Railway Environments using a Hybrid Vector Parabolic Equation/ Ray-Tracing Method, 2015 IEEE International Symposium on Antennas and Propagation & USNC/URSI National Radio Science Meeting, pp. 1680-1681, 19-24 July 2015.

Xuesong Cai, Xuefeng Yin, and Yongyu He, Weiming Duan and Silvia Ruiz Boqué, Measurement-based Stochastic Models for Channel Transistion in Undergound Subway Enviroments, 9th European Conference on Antennas and Propagation (EuCAP), 13-17 April 2015.